www.vbripress.com/aml, DOI: 10.5185/amlett.2016.6172 Published online by the VBRI Press in 2016

Microstructural and dielectric investigations of vanadium substituted barium titanate ceramics

Aditya Jain[1], Neelam Maikhuri[1], Rakesh Saroha[1], Mukul Pastor[2], A. K. Jha[3], A. K. Panwar[1*]

[1]*Department of Applied Physics, Delhi Technological University, Delhi 110042, India*

[2]*Department of Physics, Bundelkhand University, Jhansi 284002, Uttar Pradesh, India*

[3]*Department of Applied Science, A.I.A.C.T.R, Delhi 110031, India*

*Corresponding author: Tel: (+91) 9891778307; E-mail: amrish.phy@dce.edu and panwaramar@gmail.com

Received: 15 September 2015, Revised: 19 February 2016 and Accepted: 20 May 2016

ABSTRACT

In this investigation, the microstructural and dielectric properties of pure $BaTiO_3$ and vanadium (V^{5+}) substituted on Ba^{2+} site (A-site) and Ti^{4+} site (B-site) in $BaTiO_3$ ceramic have been studied. The three compositions of $BaTiO_3$ (BT), $Ba_{0.9}V_{0.1}TiO_3$ (BTA) and $BaTi_{0.9}V_{0.1}O_3$ (BTB) were synthesized using solid-state reaction route. The XRD analysis of all three compositions has been carried out at room temperature and proper phase formation for BT, BTA and BTB are confirmed. However, compositions BTA and BTB indicate the presence of secondary phases, and it may be due to higher amount of vanadium substitution at A and B sites. Addition of vanadium inhibited the grain growth of $BaTiO_3$ ceramic. Vanadium substitution on A- and B-site have resulted in decrease of Curie temperature as well as dielectric loss compared to pure BT. A more diffused behavior is observed in vanadium substituted samples as compare to pure BT which shows a sharp transition and lower value of diffuseness parameter. Impedance study shows that substitution of vanadium on A- as well as B-site results in decrease of AC conductivity. These properties of vanadium substituted samples can be utilized to reduce the dielectric loss in capacitors and in radio frequency applications.

Keywords: Barium titanate; conductivity; dielectric constant; sintering.

Introduction

Lead-based oxide materials such as lead titanate ($PbTiO_3$), lead zirconate ($PbZrO_3$), lead strontium titanate ($PbSrTiO_3$) etc. are dominant ferroelectric materials due to their extraordinary dielectric properties. Due to their inherent dielectric properties, they are widely used in sensors, actuators and multi-layered ceramic capacitor (MLCC) applications [**1**]. Although, Lead based materials contains a higher amount of lead oxide which is highly toxic and causes various environmental problems and health risks [**2-4**]. Hence, for environmental safety issues and technological advancement, research work is explored in lead-free materials such as $BaTiO_3$, $SrTiO_3$, etc. [**5**]. Barium titanate has attracted a lot of attention because of its high dielectric constant and excellent piezoelectric and pyro-electric properties. Generally, barium titanate based ceramics show sharp peak transitions, due to this reason barium titanate based materials have higher ferroelectricity compared to other perovskite structure based materials [**6-8**]. Also barium titanate based ceramics have the advantage of better electrical properties at room temperature including good chemical and mechanical stability. Pure barium titanate and its doping with certain dopants exhibit positive temperature coefficient of resistivity (PTCR) properties. This suggests that at Curie temperature it will exhibit an increase in resistance. This increase in resistance may be of several orders of magnitude. This property of barium titanate based materials can be used in sensing applications [**9**].

Barium strontium titanate is one of the preferred materials for tunable applications, but due to its high dielectric loss, it has limited applicability. In general, the substitution of transition metals and rare earths has been widely explored to improve the dielectric and microstructural properties of barium titanate ceramics [**10-11**]. It has also been observed that the substitution of non-ferroelectric material may result in decrease in dielectric constant as well as the dielectric loss [**12, 13**]. Nagao *et al.* [**14**] have synthesized Eu-doped $BaTiO_3$ nanoparticles by hydrolysis and found an enhancement in luminescent properties and dielectric properties. Nath *et al.* [**15**] prepared bismuth doped $BaTiO_3$ by solid state reaction and found an enhancement in piezoelectric properties. Petrovic *et al.* [**16**] found the addition of La results in increase of dielectric constant and appearance of PTCR effect in barium titanate ceramic. Liu *et al.* [**17**] showed that cobalt doping in barium titanate may results in better ferromagnetic properties and can be used for multiferroic applications. It is implied that proper doping or substitution can improve microstructural, electrical and magnetic properties of $BaTiO_3$ ceramics. Vanadium is one of the most important dopant and have resulted in modifying microstructural and dielectric properties of various

ceramics. Moreover, it is well reported that electrical behavior of barium titanate based ceramics is related to chemical state of the constituent materials [**18**]. In recent years, most studies are concentrated on temperature dependence of the dielectric properties, magnetic, optical, relaxor behavior and domain structure of barium titanate based materials. Zheng *et al*. [**19**] reported that vanadium substitution at B-site could enhance ferroelectric properties of $CaBi_4Ti_4O_{15}$ ceramic. Effects of vanadium doping on dielectric properties in barium strontium titanate and strontium bismuth niobate have been investigated by Bandyopadhyay et al. [**20**] and Wu *et al*. [**21**]. However, there is no information on the microstructure and electrical properties of higher amount of vanadium doping in barium titanate ceramics, which prompted the authors to investigate the present composition.

The objective of this research is to investigate the effect of higher amount of vanadium substitution on A- and B-site of $BaTiO_3$ ceramic and analyze their microstructural, dielectric and impedance properties. In addition, the temperature dependence of the dielectric constant was used to evaluate the diffuseness parameter for comprehending the modulation in ferroelectric transition characteristics due to the vanadium substitution on A- and B-site.

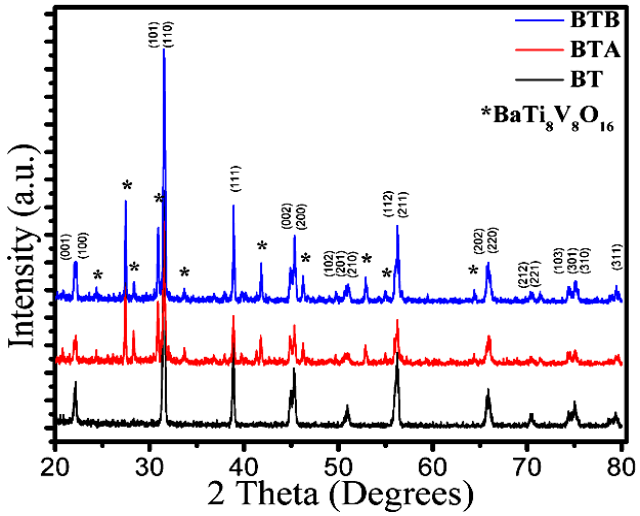

Fig. 1. XRD patterns of BT1260, BTA1200 and BTB1200 ceramics pellets sintered for 4 hours.

Experimental

Synthesis of ceramics

$BaTiO_3$ (BT), $Ba_{0.9}V_{0.1}TiO_3$ (BTA) and $BaTi_{0.9}V_{0.1}O_3$(BTB) were synthesized using solid-state reaction route. The starting materials barium carbonate ($BaCO_3$, 99.0%, Sigma-Aldrich), titanium oxide (TiO_2, 99.9%, Sigma-Aldrich) and vanadium pentoxide (V_2O_5, 99.9%, Merck Millipore) were used to synthesize the desired compositions. These precursors were thoroughly mixed and grounded in mortar-pestle for approximately 5 hours and then all the three compositions were calcined at 1100°C for 4 hours to remove volatile impurities. The calcined powders were mixed with 2.5 wt.% poly-vinyl alcohol and then they were pressed into pellets at 50 MPa pressure. These pellets were kept at 220°C for 40 min to eliminate the solvent and binder after that these pellets were sintered at different temperatures. The pure barium titanate (BT) powder was sintered at 1225°C and 1260 °C for 4 hours. While vanadium substituted compositions, BTA and BTB were sintered at 1150 °C and 1200 °C for 4 hours.

Characterization

Phase formation of pure BT, BTA and BTB were analyzed using X-ray diffractogram recorded by Bruker D8 Advance X-ray diffractometer using $CuK_{\alpha 1}$ radiation of wavelength, 1.540 Å in conjunction with Ni filter. Microstructural analysis of the specimens was done by using Hitachi S-3700 scanning electron microscope. Dielectric measurements were performed to observe the effect of variation of dielectric constant and dielectric loss with temperature and frequency using Agilent 4284A precision LCR meter on a polished and silver coated pellets of size 10 mm diameter and 1 mm thickness. The measurements were performed in the temperature range of 27° C to 190° C.

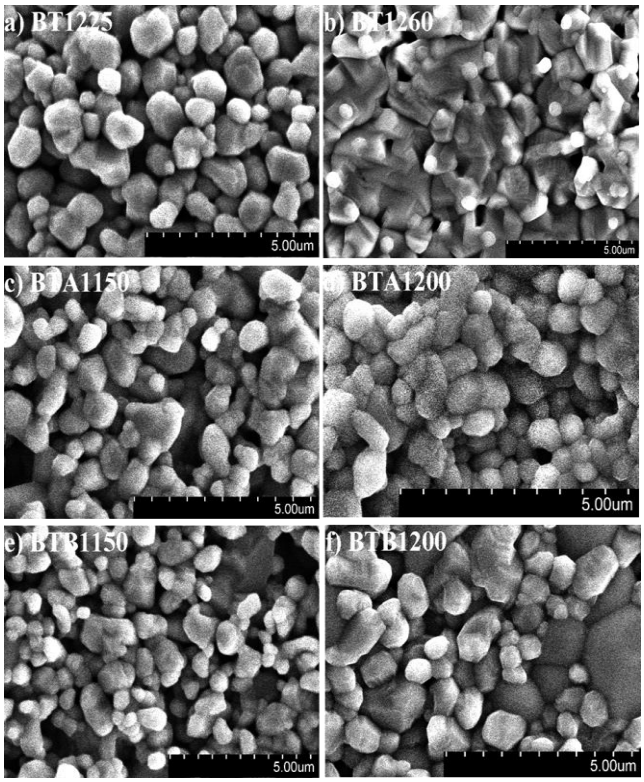

Fig. 2. SEM micrograph of compositions of ceramics sintered at different temperatures for 4 hours: (i) pure BT (a): 1225°C and (b): 1260°C; (ii) BTA (c): 1150 °C and (d): 1200 °C; (iii) BTB (e): 1150 °C and (f): 1200 °C.

Results and discussion

Crystal structure

X-ray diffraction pattern of pure BT specimen sintered at 1260 °C for 4 hours (BT1260), BTA and BTB both sintered at 1200 °C for 4 hours (BTA1200 and BTB1200) ceramics are shown in **Fig. 1**. These XRD patterns were indexed with standard barium titanate compound (JCPDS no. – 01-075-0462) using X'pert highscore software, which

confirms the formation of tetragonal phase with P4mm space group for pure BT. However, some extra peaks (marked as *) are also observed in the patterns of BTA and BTB. Peaks marked as * are identified as secondary phase, possibly due to higher amount of substitution of vanadium in BTA and BTB and they belong to $BaTi_8V_8O_{16}$ having tetragonal phase with I4/m space group. The XRD patterns also indicate that irrespective of vanadium substitution on A site or B site, the vanadium ion might have gone to the same site in both the compositions. The presence of non-ferroelectric secondary phases in XRD pattern of BTA and BTB may lead to a decrease in dielectric constant [**22-25**].

Microstructural analysis

Fig. 2 shows the SEM images of all the three samples sintered at different temperatures. To see the effect of sintering temperature on the microstructural properties of ceramics, all the three compositions were sintered at two different temperatures. The pellets of pure barium titanate composition were sintered at 1225 °C and 1260 °C. It is observed that BT sample sintered at 1225°C (BT1225) possess a uniform distribution of grains with clearly visible grain boundaries. While the BT sample sintered at 1260 °C (BT1260) shows some agglomeration in grains. The average grain size of BT1225 sample is observed to be in the range of 750 to 780 nm as calculated from Image J software. The vanadium substituted compositions BTA and BTB were sintered at three different sintering temperatures: 1150°C, 1200°C and 1225°C. The reason for low-temperature synthesis of vanadium substituted samples is the lower melting point of vanadium precursor (V_2O_5), which results in melting of overall composition [**26**].

It is observed that up to sintering temperature of 1200 °C vanadium substituted samples BTA1200 and BTB1200 retain the visible grains and grain boundaries, while for sintering temperature above 1200 °C both vanadium substituted compositions have started melting. The average grain size of BTA1150, BTB1150, BTA1200 and BTB1200 were found to be in the range of 510-530 nm, 535-550 nm, 490-515 nm and 570-590 nm, respectively. Hence, the average grain size of both the vanadium substituted compositions decreases as compare to pure BT. These results also suggest that the decrease in average grain size of vanadium substituted compositions may lead to decrease in dielectric constant [**27**].

Dielectric study

Dielectric measurements of all three compositions BT1260, BTA1200 and BTB1200 were performed. The temperature dependence of dielectric constant and dielectric loss of these three compositions at three frequencies measured in the temperature range of 27 to 200 °C are shown in **Fig. 3(a)-(c)**. It can be seen from **Fig. 3** that at lower temperature the dielectric constant decreases gradually and near the Curie temperature the dielectric constant increases abruptly and then decreases indicating the phase transition from ferroelectric state to paraelectric state [**28, 29**]. The decrease in dielectric constant above T_c is due to the structural transition from tetragonal to cubic phase. Moreover, there is an increase in thermal oscillations of the molecules and degree of disorder in dipoles in cubic phase, which results in decrease of dielectric constant [**30**]. It is observed that as frequency increases dielectric constant decreases, this may be because the increase in frequency leads to a drop in net polarization of the material. Overall the magnitude of dielectric constant decreases in vanadium substituted compositions BTA and BTB. The higher value of dielectric constant for pure BT as compare to vanadium substituted samples may be due to well-developed grains which result in the easier motion of the domain walls [**31**].

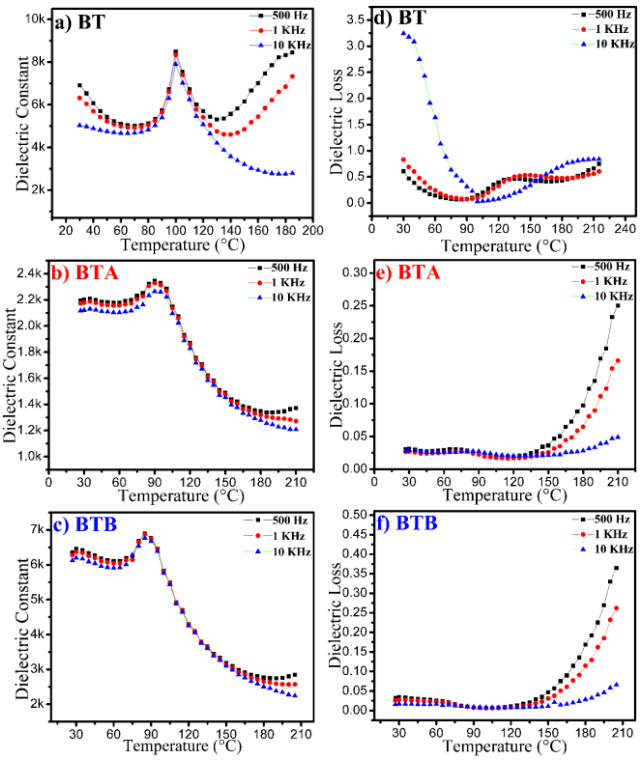

Fig. 3. Variation of dielectric constant and dielectric loss with temperature: (a) and (d) for BT1260; (b) and (e) BTA1200; (c) and (f) BTB1200 at three different frequencies of 500Hz, 1KHz and 10KHz.

Dielectric loss of all three compositions, BT1260, BTA1200 and BTB1200 at different frequencies, 500 Hz, 1 kHz, and 10 kHz are shown in **Fig. 3(d)-(f)**. It has been observed that the dielectric loss of pure BT is much higher at lower temperature (room temperature), as the temperature increases the dielectric loss decreases upto 100°C and again increases further after crossing dielectric transition temperature. It can be seen that the magnitude of dielectric loss in the observed temperature range of 27 °C to 210 °C is lower in BTA and BTB compared to that in BT. The dielectric loss remains almost constant in the vanadium substituted compositions BTA and BTB from room temperature to 150 °C temperature at different frequencies of 500 Hz, 1 kHz and 10 kHz. A sharp increase in the dielectric loss is observed at higher temperatures in BTA and BTB specimens. The increase in dielectric loss at higher temperature and high frequencies may be due to the increase in the mobility of charge carriers arises from the vacancies or defects in of BTA and BTB compositions [**32**]. A decrease in dielectric loss in BTA and BTB specimen compared to pure BT is observed which may be attributed to charge compensation effect caused by the substitution of V^{5+} on A and B site of $BaTiO_3$ structure. The

variation of dielectric constant and dielectric loss is also observed in a wide range of frequency range of 20 Hz to 1 MHz, as shown in **Fig. 4**. The measurements were taken at three different temperatures of 30 °C, 100 °C and 175 °C. It is observed that vanadium substituted BTA and BTB samples show almost similar behavior for dielectric constant and dielectric loss except that BTA has lower value of both the dielectric constant and dielectric loss. Overall on comparing both the dielectric constant and dielectric loss with frequency in BT, BTA and BTB for different temperatures, it is observed that BTA has lower dielectric loss compared to BT and BTB. Similar behavior is noticed in case of dielectric constant in terms of overall magnitude.

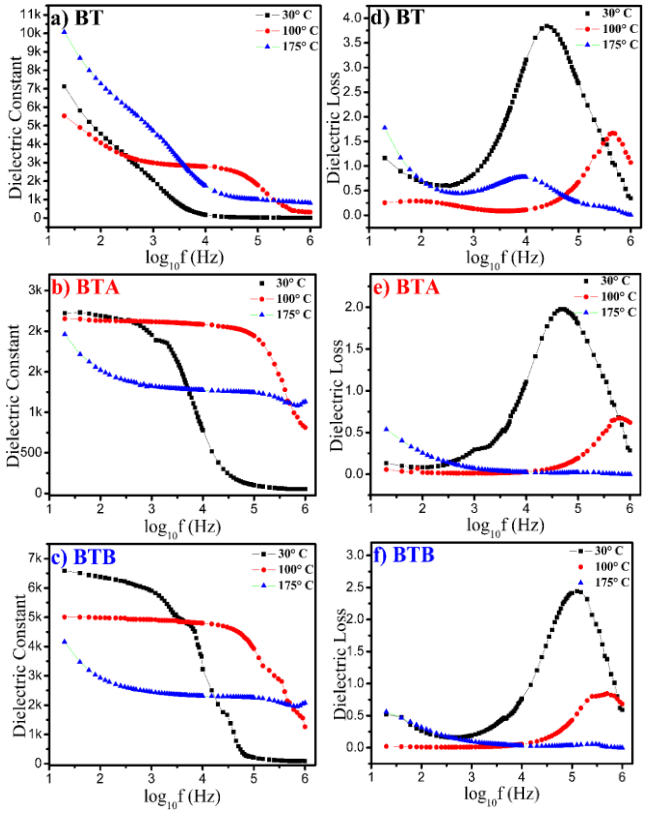

Fig. 4. Variation of dielectric constant and dielectric loss with frequency: (a) and (d) BT1260; (b) and (e) BTA1200; (c) and (f) BTB1200 at three different temperatures of 30 °C, 100 °C and 175 °C.

The variation of dielectric constant with temperature is also related to the tolerance factor of perovskite materials. The tolerance factor can be calculated from the following equation [33-35]:

$$t = \frac{R_O + R_A}{\sqrt{2}(R_B + R_O)} \quad (1)$$

where, R_A is the ionic radius of A site atom, R_B is ionic radius of B site atom and R_O ionic radius of the oxygen atom. But above equation is modified for the compositions of BTA and BTB of vanadium substituted compositions in this investigation and it may be rewritten as:

For A site:

$$t = \frac{R_O + (0.9R_{Ba^{2+}} + 0.1R_{V^{5+}}}{\sqrt{2}(R_{Ti^{4+}} + R_O)} \quad (2)$$

For B site:

$$t = \frac{R_O + R_{Ba\,2+}}{\sqrt{2}(0.9R_{Ti\,4+} + 0.1R_{V\,5+} + R_O)} \quad (3)$$

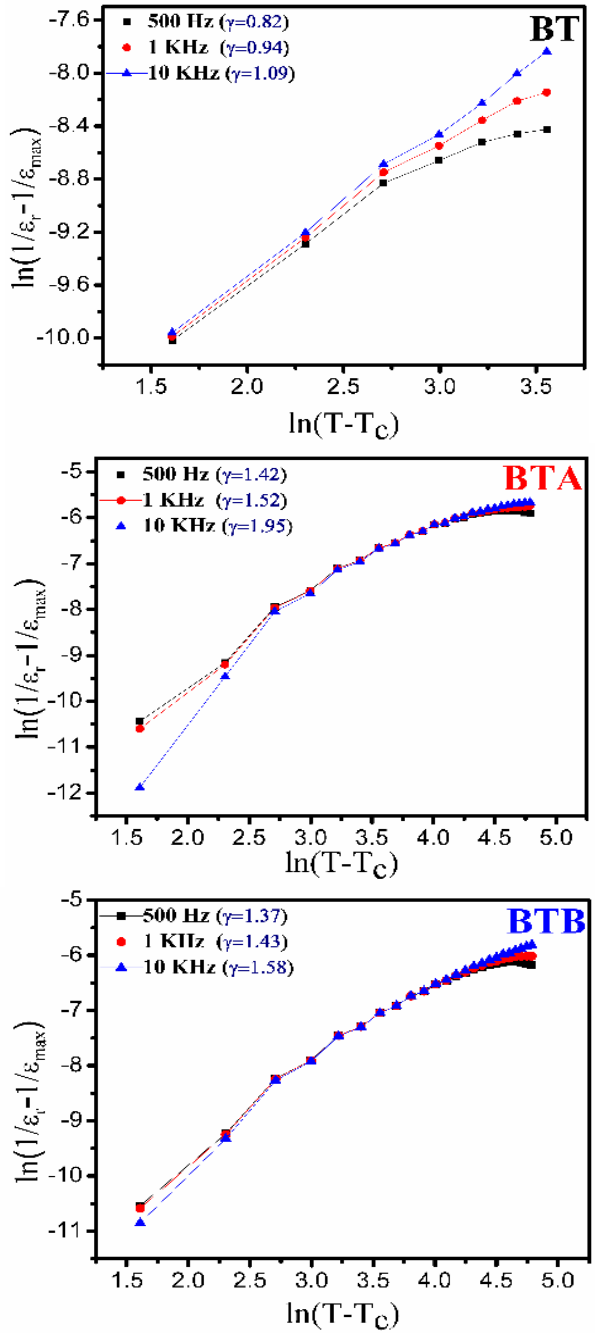

Fig. 5. Diffuseness parameter for BT1260, BTA1200 and BTB1200 at 500Hz, 1KHz and 10KHz.

For stable perovskite structure, value of t should be close to unity. The value of tolerance factor for BTA and BTB were found to be 1.023 and 1.065 compared to 1.061 for pure BT. Pure BT possesses a stable ferroelectric phase with sharp phase transition while a little deviation from its tolerance value has resulted in disorderedness in the

material leading to diffuse transition as observed in BTA and BTB. The diffuseness of phase transition γ was calculated for all the three compositions and is shown in **Fig. 5**. The empirical relation of diffuseness parameter is given by following equation for a modified Curie-Weiss law [**36-38**].

$$\frac{1}{\varepsilon} - \frac{1}{\varepsilon_m} = \frac{(T-T_c)^{\gamma}}{C'} \quad (4)$$

where, ε is the dielectric constant, ε_m is the dielectric constant at temperature T_c, c' is the curie constant and γ represents the diffuseness parameter.

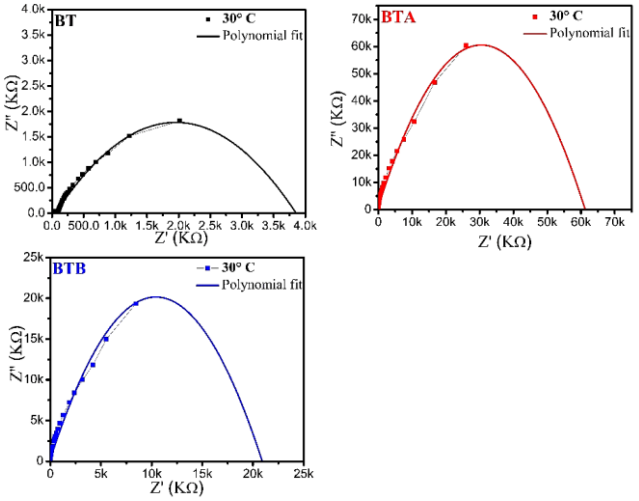

Fig. 6. Estimation of AC resistance of BT1260, BTA1200 and BTB1200 using Nyquist plot.

The diffuseness parameter, γ = 1corresponds to normal ferroelectric behavior while 1< γ<2 correspond to diffused phase transition [**39-41**]. The value of diffuseness parameter was calculated for BT, BTA and BTB compositions at three different frequencies 500 Hz, 1 kHz and 10 kHz. A higher value of diffusivity was observed for BTA and BTB leading to lower ferroelectricity compared to that in BT. A higher value of diffusivity also suggests that on substitution of vanadium ion on A and B site of BT lattice have resulted in the lowering of long range ordering and crystallinity of the material [**42**]. The ionic radii of Ti^{4+} and V^{5+} in six coordination no. are 60.5 and 54 pm, respectively as compare 135 pm for Ba^{2+}. This suggest the higher probability of vanadium ion to go on to Ti site rather than at Ba site, also a much higher charge compensation is required at Ba site rather than at Ti site for vanadium substitution.

Impedance study

Impedance measurement was carried out at room temperature in the frequency range 20 Hz-1 MHz. Fig. 6 shows the Nyquist plot between real (Z') and imaginary (Z'') parts of the impedance for the synthesized specimens BT, BTA and BTB. Nyquist plots for BT, BTA and BTB indicate generation of only one semicircle which corresponds to the grain boundary resistance. However, grain boundary resistance is maximum in BTA while minimum in pure BT suggesting that there is decrease in conductivity when vanadium is substituted either at A-site or B-site while for BTB it is lower than BTA means vanadium substitution is more favorable at B-site rather than A-site. It is found that AC conductivity decreases with vanadium substitution in BTA and BTB compositions. The obtained value of conductivity for BT, BTA and BTB are 5.07, 0.34 and 0.95 μS/m, respectively. The decrease in conductivity of BTA and BTB compared to that in pure BT may be due to the higher number of grain boundaries in vanadium substituted samples because higher no. of grain boundaries contributes to grain boundary resistance which further result in the form of overall resistance [**43**].

Conclusion

$BaTiO_3$(BT), $Ba_{0.9}V_{0.1}TiO_3$(BTA) and $BaTi_{0.9}V_{0.1}O_3$(BTB) were synthesized by solid state reaction route. X-ray diffraction pattern confirms the tetragonal phase for all the three samples BT, BTA and BTB while secondary peaks of $BaTi_8V_8O_{16}$ for BTA and BTB was also observed, which suggests the limited solubility of vanadium in barium titanatelattice. Micro structural investigation indicates that addition of vanadium has inhibited the grain growth and results in decrease of grain size compared to pure BT. The sintering temperature of pure BT was reduced by approximately 60-80 °C with vanadium substitution. The addition +of vanadium causes the lowering in the Curie temperature. The dielectric constant of the ceramic was found to decrease, which is due to decrease in crystallinity and presence of non-ferroelectric secondary phase with vanadium substitution. The diffuseness of phase transition enhances with vanadium substitution on A- and B-site of $BaTiO_3$. The substitution of higher concentration of vanadium on Ba^{2+} and Ti^{4+} results in decrease of dielectric constant which may be attributed to decreased leakage current inside the material. AC conductivity results shows that vanadium substituted samples possesses a lower value of conductivity that can be correlated to grain boundary effect which is dominating in BTA and BTB as compared to BT. The lowering of dielectric loss and conductivity of the material can be utilized in fabricating the multi-layered ceramic capacitors (MLCC), radio frequency applications and in reducing dielectric materials losses.

Reference

1. Moulson, A. J. and Herbert, J. M., *Electroceramics:* Dielectrics and Insulators; *Wiley*, **2003**, *pp.* 243. **DOI:** 10.1002/0470867965.ch5
2. K. Takeda, T. Muraishi, T. Hoshina, H. Takeda, and T. Tsurumi, *J. Appl. Phys.***2010,** *107*, 074105. **DOI:** 10.1063/1.3371679
3. L.G.A. Marques, L.S. Cavalcante , A.Z. Sim˜oes , F.M. Pontes , L.S. Santos-J´unior, M.R.M.C. Santos, I.L.V. Rosa , J.A. Varela , E. Longo, *Mater. Chem. Phys.***2007,** *105* 293. **DOI:** 10.1016/j.matchemphys.2007.04.065
4. X.G. Tang, R.K. Zheng, Y.P. Jiang, H.L.W. Chan, *J. Appl. Phys.* **2006**, *39*, 3394. **DOI:** 10.1088/0022-3727/39/15/026
5. W. Wang, W.L. Li, D. Xu, W.P. Cao, Y.F. Hou, W.D. Fei, *Ceramic. Inter.***2014,** *40* 3933. **DOI:** 10.1016/j.ceramint.2013.08.037
6. John Bechhoefer, Yi Deng, Joel Zylberberg, Chao Lei, and Zuo-Guang Ye, *Am J Phys.***2007,** *75*, 1046. **DOI:** 10.1119/1.2723801

7. LaviniaCurecheriu, Maria Teresa Buscaglia, Vincenzo Buscaglia, Zhe Zhao, and Liliana Mitoseriu, *Appl. Phys. Lett.* **2010,** *97*, 242909. **DOI:** 10.1063/1.3526375
8. J. Zhang, M. W. Cole, and S. P. Alpay, *J. Appl. Phys.* **2010,** *108*, 054103. **DOI:** 10.1063/1.3475482
9. Wei Cai, Chunlin Fu, JiachengGao, Xiaoling Deng, Weihai Jiang and Zebin Lin, *Mater. Sci. Forum* **2011,** *687*, 263. **DOI:** 10.4028/www.scientific.net/MSF.687.263
10. Ansu Kumar Roy, K. Amar Nath, K. Prasad, Ashutosh Prasad, *Adv. Mater. Lett.* **2014,** *5(2)*,100. **DOI:** 10.5185/amlett.2013.fdm.77
11. Neelam Maikhuri, Amrish K. Panwar, A. K. Jha, *J. Appl. Phys*. 2013, 113, 17D915. **DOI:** 10.1063/1.4796193
12. Su-E Hao, Liang Sun, Jin-Xiang Huang, *Mater. Chem. Phys.* **2008,** *109*, 45. **DOI:** 10.1016/j.matchemphys.2007.10.041
13. Wei Cai, Chunlin Fu, Zebin Lin, Xiaoling Deng, *Ceram. Int.* **2011**, 37, 3643. **DOI:** 10.1016/j.ceramint.2011.06.024
14. Daisuke Nagao, Hirobumi Saito, Haruyuki Ishii, Yoshio Kobayashi, Mikio Konno, *Colloids Surf. A* **2012**, 409, 94. **DOI:** 10.1016/j.colsurfa.2012.05.042
15. A.K. Nath, Nirmali Medhi, *Mater. Lett.***2012**, 73, 75. **DOI:** 10.1016/j.matlet.2011.12.113
16. M.M. VijatovićPetrović, J.D. Bobić, T. Ramoška, J. Banys, B.D. Stojanović, *Mater. Charact.* **2011**, 62, 1000. **DOI:** 10.1016/j.matchar.2011.07.013
17. Hongxue Liu, Baobao Cao, Charles J. O'Connor, *J. Magn. Magn. Mater.***2010**, 322, 790. **DOI:** 10.1016/j.jmmm.2009.11.004
18. Chunlin Fu, Jingnan Liang, Wei Cai, Gang Chen, Xiaoling Deng, *J. Mater. Sci. - Mater. Electron.***2013**, 24, 2438. **DOI:** 10.1007/s10854-013-1115-4
19. Jiangtao Zeng, Yongxiang Li, Qunbao Yang, Qingrui Yin, Mater. Sci. Eng., B **2005**, 117, 241-245. **DOI:** 10.1016/j.mseb.2004.11.015
20. S. Bandyopadhyay, S.J. Liu, Z.Z. Tang, R.K. Singh, N. Newman, *Acta Mater.* **2009**, 57, 4935–4947. **DOI:** 10.1016/j.actamat.2009.06.063
21. Yun Wu, Chau Nguyen, SeanaSeraji, Mike J. Forbess, Steven J. Limmer, Tammy Chou, Guozhong Cao, *J. Am. Ceram. Soc.* **2001**, 84, 2882-88. **DOI:** 10.1111/j.1151-2916.2001.tb01109.x
22. Xiujian Chou, Jiwei Zhai, W and Xi Yao, *J. Am. Ceram. Soc.***2007,** *90*, 2799–2801. **DOI:** 10.1111/j.1551-2916.2007.01825.x
23. Kumari, M.; Prakash, C.; and Chatterjee, R.; *J. Appl. Phys.* **2013,** *113*, 17D918. **DOI:** 10.1063/1.4795425
24. Daniel J. R. Appleby, Nikhil K. Ponon, Kelvin S. K. Kwa, SrinivasGanti, UllrichHannemann, Peter K. Petrov, Neil M. Alford, and Anthony O'Neill, *J. Appl. Phys.* **2014,** *116*, 124105. **DOI:** 10.1063/1.4895050
25. Wei Cai, Jiacheng Gao, Chunlin Fu, Liwen Tang, *J. Alloy. Comp.* **2009,** *487*, 668–674. **DOI:** 10.1016/j.jallcom.2009.08.034
26. Lai, George Y.; *High-Temperature Corrosion and Materials Applications ASM International*, **2007**. **ISBN:** 978-0-87170-853-3
27. S. Bhaskar Reddy, K. Prasad Rao, M.S. Ramachandra Rao," *J. Alloy. Comp.* **2014,** *509*, 1266. **DOI:** 10.1016/j.jallcom.2010.09.211
28. Yuanliang Li, Ranran Wang, Xuegang Ma, Zhongqiu Li, Rongli Sang, Yuanfang Qu, *Mater. Res. Bull.***2014,** *49*, 601. **DOI:** 10.1016/j.materresbull.2013.10.001
29. P. Mishra a, Sonia b, P. Kumar, *J. Alloy. Comp.* **2012,** *545*, 210. **DOI:** 10.1016/j.jallcom.2012.08.017
30. Kumar, N.; Tirupathi, P.; Kumar, B.; Pastor, M.; Pandey, A. C.; Choudhary, R. N. P.; *Adv. Mater. Lett.* **2015,** *6(4)*, 284**.** **DOI:** 10.5185/amlett.2015.6618
31. Wei Han, Zhu, J.; Sijia Zhang, Zhang Hui, Xiaohui Wang, Qinglin Wang, ChunxiaoGao, and Changqing Jin, *J. Appl. Phys.* **2013,** *113*, 193513. **DOI:** 10.1063/1.4806996
32. Priyanka Arora Jha, A.K. Jha, *J. Alloy. Comp.* **2012,** *513*, 580. **DOI:** 10.1016/j.jallcom.2011.11.012
33. Priyanka A. Jha, A.K. Jha, *Ceramic. Inter.* **2014,** *40*, 5209. **DOI:** 10.1016/j.ceramint.2013.10.087
34. M. Ganguly, S.K. Rout, C.W. Ahn , I.W. Kim, ManoranjanKar, Structural, *Ceramic. Inter.* **2013,***39*, 9511-9524. **DOI:** 10.1016/j.ceramint.2013.05.070
35. T. Limboeck and E. Soergel, *Appl. Phys. Lett.***2014,** *105*, 152901. **DOI:**10.1063/1.4897361
36. Xia Huang, Jingji Zhang, LudongJi, Hongfang Qi, Jiangying Wang, *J. Alloy. Comp.* **2014,** *592*, 105–108. **DOI:** 10.1016/j.jallcom.2014.01.015
37. P. A Jha and A K Jha, *Indian J. Phys.***2014,** *88(5)*, 489-496. **DOI:** 10.1007/s12648-014-0445-2
38. E. Antonelli, M. Letonturier, J.-C. M'Peko , A.C. Hernandes, *J. Eur. Ceram. Soc.***2009,** *29*, 1449–1455. **DOI:** 10.1016/j.jeurceramsoc.2008.09.009
39. PatriTirupathi, Nawnit Kumar, Mukul Pastor, A. C. Pandey and R. N. P. Choudhary*J. Appl. Phys*. **2015**, *117* , 074105. **DOI:** 10.1063/1.4908222
40. JianQuan Qi , Bai Bo Liu , Hu Yong Tian , Han Zou , Zhen Xing Yue, Long Tu Li, *Solid State Sci.***2012,** *14*, 1520-1524. **DOI:**10.1016/j.solidstatesciences.2012.08.009
41. Andreas Leschhorn, StephaneDjoumbou, and Herbert Kliem, *J. Appl. Phys.* **2014,** *115*, 114106. **DOI:**10.1063/1.4868901
42. S. Bhagat, K. Amar Nath, K.P. Chandra, R.K. Singh, A.R. Kulkarni, K. Prasad, *Adv. Mater. Lett.* **2014**, *5(3)*, 117-121. **DOI:**10.5185/amlett.2013.fdm.28
43. DevidasGulwade, Prakash Gopalan, *Physica B***2009**, *404*, 1799-1805. **DOI:** 10.1016/j.physb.2009.02.026

Graphical abstract